

RESEARCH

Open Access



Development of differential diagnostic models for distinguishing between limb-girdle muscular dystrophy and idiopathic inflammatory myopathy

Guangyu Wang¹, Lijun Fu², Lining Zhang³, Kai Shao⁴, Ying Hou¹, Tingjun Dai¹, Pengfei Lin¹, Chuanzhu Yan^{1,5} and Bing Zhao^{1,5*}

Abstract

Objective Limb-girdle muscular dystrophy (LGMD) is usually confused with idiopathic inflammatory myopathy (IIM) in clinical practice. Our study aimed to establish convenient and reliable diagnostic models for distinguishing between LGMD and IIM.

Methods A total of 71 IIM patients, 24 LGMDR2 patients and 22 LGMDR1 patients diagnosed at our neuromuscular center were enrolled. Differences in clinical, laboratory and histopathological characteristics were comprehensively compared. A nomogram and a decision tree were developed to distinguish between LGMD and IIM patients.

Results Compared to patients with LGMD, IIM patients exhibited a significantly older age of onset, a higher prevalence of cervical flexor weakness and a more commonly diffuse MHC-I expression on muscle pathology. The ratio of synchronous serum myoglobin (Mb, ng/ml) to creatine kinase (CK, U/L) before immunotherapy was significantly higher in IIM patients than in LGMD patients. Receiver operating characteristic analysis indicated a high differential diagnostic efficiency of synchronous Mb/CK with a cutoff value of 0.18. A nomogram prediction model and a decision tree were developed based on four independent indicators (age of onset, cervical flexor weakness, synchronous Mb/CK and diffuse MHC-I expression). Five-fold cross-validation and bootstrapping techniques substantiated the discriminate efficacy of the nomogram and decision tree.

Conclusion We developed two practical differential diagnosis models for LGMD and IIM based on the analysis of four accessible indicators, including the age of onset, cervical flexor weakness, the ratio of synchronous Mb/CK values and diffuse MHC-I expression. Further studies with larger samples are needed to refine the predictive efficiency of the differential diagnostic models.

Keywords Necrotizing myopathy, Idiopathic inflammatory myopathy, Limb-girdle muscular dystrophy, Myoglobin, Creatine kinase

*Correspondence:

Bing Zhao

zhaobing1122@126.com

Full list of author information is available at the end of the article



© The Author(s) 2024. **Open Access** This article is licensed under a Creative Commons Attribution-NonCommercial-NoDerivatives 4.0 International License, which permits any non-commercial use, sharing, distribution and reproduction in any medium or format, as long as you give appropriate credit to the original author(s) and the source, provide a link to the Creative Commons licence, and indicate if you modified the licensed material. You do not have permission under this licence to share adapted material derived from this article or parts of it. The images or other third party material in this article are included in the article's Creative Commons licence, unless indicated otherwise in a credit line to the material. If material is not included in the article's Creative Commons licence and your intended use is not permitted by statutory regulation or exceeds the permitted use, you will need to obtain permission directly from the copyright holder. To view a copy of this licence, visit <http://creativecommons.org/licenses/by-nc-nd/4.0/>.

Introduction

Necrotizing myopathies represent a spectrum of diseases, which could be caused by various hereditary or autoimmune conditions. Limb-girdle muscular dystrophy (LGMD) and idiopathic inflammatory myopathy (IIM) are recognized as the two most common prototypes of necrotizing myopathies. Theoretically, it is easy to diagnose a patient with LGMD based on a definitive gene mutation and the concomitant reduction of the aberrant sarcolemmal protein as observed on muscle pathology. Otherwise, it is more supportive of IIM if the patient has a positive myositis-specific autoantibody (MSA) and a favorable response to immunotherapy. However, it is estimated that approximately 50% of patients suspected of having LGMD could not be genetically confirmed through whole exome sequencing [1, 2]. In the case of IIMs, MSAs could be negative in 30–40% of patients [3–5], and an inadequate response to a sufficient immunosuppressive regimen does not exclude the diagnosis of refractory IIM, especially in those with a long disease duration [6, 7].

Several previous studies have compared the different characteristics of LGMD and IIM patients. An early study focusing on juvenile polymyositis and muscular dystrophy revealed that complex repetitive discharges on electromyography were more common in the former condition, while muscle atrophy on magnetic resonance imaging (MRI), as well as myofiber hypertrophy and fibrosis on muscle biopsy were more indicative of the latter condition [8]. A recent study compared the clinicopathological distinctions between LGMDR2 and immune-mediated necrotizing myopathy (IMNM) [9]. The findings suggested that LGMDR2 is more likely to manifest without cervical muscle weakness or dysphagia, less myalgia, and no extramuscular organs involvement (except for the heart). In addition, muscle biopsies frequently demonstrate the presence of whorled, ring, or splitting myofibers in LGMDR2. In contrast, adductor magnus edema on MRI was a distinguishing feature of IMNM [9]. Another pathological study reported that inflammatory features, such as lymphocyte infiltration, major histocompatibility complex class-I (MHC-I) expression, and membrane attack complex (MAC) deposition, were useful only for distinguishing LGMD from dermatomyositis (DM) and sporadic inclusion body myositis (sIBM) [10]. Although the aforementioned experiences exist, it is still challenging but imperative to distinguish between muscular dystrophy (MD) patients and IIM patients, as it is critical for determining the appropriateness of long-term immunotherapy and the potential need for a more aggressive regimen in patient who exhibit unfavorable responsiveness.

We observed some significant differences in the clinical and muscle pathological characteristics between patients

with LGMD and IIM. Interestingly, we also found a significant difference in the ratio of synchronous myoglobin (Mb) to CK between the two conditions. Furthermore, we attempted to establish a practical differential diagnostic model for distinguishing between LGMD and IIM.

Materials and methods

Patients

This was a retrospective observational study at our neuromuscular disorder (NMD) center. As dysferlinopathy (LGMDR2) and calpainopathy (LGMDR1) are presently recognized as the two most common forms of LGMD, which are frequently confused with IIM [11]. To minimize the heterogeneity among enrolled patients, this study exclusively included individuals diagnosed with LGMDR1 and LGMDR2 to serve as representatives of LGMD.

The inclusion criteria for patients with necrotizing myopathy were as follows: (1) limb-girdle pattern of weakness; (2) peak creatine kinase (CK) > 1000 U/L; (3) necrotic myopathic changes on muscle pathology, plus one of the following features: (1) a positive result of MSA test and/or definite response to immunotherapy, which will be included in the IIM group; (2) sarcolemma reduction of dysferlin protein expression on muscle pathology and pathogenic compound heterozygous mutations in the *DYSF* gene identified by genetic analysis, which will be included in the LGMDR2 group; and (3) pathogenic compound heterozygous mutations in the *CAPN3* gene identified by genetic testing, which will be included in the LGMDR1 group. There are several pathognomonic characteristics of IIM patients, so the exclusion criteria are as follows: (1) the presence of DM-skin rashes; (2) perifascicular changes, including perifascicular atrophy, perifascicular necrosis or perifascicular MHC-I/II expression on muscle pathology; and (3) sIBM. A total of 24 LGMDR2 patients and 22 LGMDR1 patients who were ever diagnosed at our NMD center between April 2009 and September 2023 and 71 IIM patients between April 2021 and September 2023 were enrolled in this study. One of the LGMDR1 patients did not undergo further pathological analysis, as the muscle specimen was nearly completely replaced by fatty infiltration.

Clinical and laboratory evaluation

The clinical evaluation included demographic information, medical history, and neuromuscular examinations. The serum Mb (ng/ml) /CK (U/L) ratio was recognized as an effective indicator for evaluating the risk of acute kidney injury in patients with rhabdomyolysis [12]. In the present study, serum CK and Mb values were collected simultaneously before any pharmacological intervention to assess the difference between the two subgroups. Receiver operating characteristic (ROC) analysis was

performed to determine the differential diagnostic efficiency of the ratio of synchronous Mb (ng/ml) to CK (U/L). MSAs for the IIM patients were tested by dot immunoassay (Autoimmune Myositis Profile Antibody IgG Detection Kit, MyBiotech Co., Ltd., Xi'an, China, MT559) following the manufacturer's instructions, including DM-specific antibodies (anti-Mi2, anti-MDA5, anti-TIF1 γ , anti-NXP2, anti-SAE), anti-aminoacyl tRNA synthetase (ARS) antibodies (anti-Jo-1, anti-PL-7, anti-PL-12, anti-EJ, anti-OJ, anti-KS and anti-Zo, anti-Ha), anti-SRP and anti-HMGCR antibodies. For LGMD patients, gene mutations were identified based on next-generation sequencing technology.

Histopathological examinations

Pretreatment open-muscle biopsies were conducted on all patients for diagnostic purposes. Routine histological and immunohistochemical staining were performed. Serial cryostat sections were stained with the following reagents: hematoxylin and eosin (HE), nicotinamide adenine dinucleotide tetrazolium reductase (NADH), cytochrome oxidase (COX), modified Gomori trichrome (MGT), anti-dysferlin monoclonal antibody (NCL-Hamlet; Novocastra), anti-MHC-I rabbit monoclonal antibody (clone EP1395Y; Abcam), anti-C5b-9 (MAC) mouse monoclonal antibody (clone aE11; Dako), anti-myxovirus resistance protein (MxA) rabbit polyclonal antibody (ab95926; Abcam), anti-CD3 mouse monoclonal antibody (clone LN10; Zhongshan Golden Bridge Biotechnology), anti-CD20 rabbit monoclonal antibody (ab78237; Abcam), and anti-CD68 monoclonal antibody (clone KP1; Zhongshan Golden Bridge Biotechnology). All biopsies were independently re-evaluated by two neurologists with specialized training in neuromuscular pathology, Tingjun Dai and Bing Zhao, who were blinded to the clinical information.

Regarding the pathological evaluation, the DM scoring system in previous studies was applied in the evaluation of necrotic myofibers and inflammatory domains [13, 14]. The presence of hypertrophic/split fibers, whorled/ring fibers, ragged red fibers (RRFs) and fibers with internalized nuclei was also recorded. Myofiber MxA expression was defined as sarcoplasmic staining of nonnecrotic myofibers. Myofiber MHC-I expression was defined as sarcolemma staining, associated or not associated with sarcoplasmic staining. Diffuse MHC-I expression was identified when the proportion of positive myofibers exceeded 80% of the entire slice field. MAC deposition on the capillaries and sarcolemma of nonnecrotic fibers was also recorded.

Statistical analysis

Categorical variables are presented as frequencies and percentages. Continuous variables with a normal

distribution are expressed as the mean \pm standard deviation, while those with a skewed distribution are represented as the median and interquartile range [M(Q1, Q3)]. For certain categorical variables, including the proportion of females, cervical muscle weakness, myalgia, bulbar symptoms, distal muscle weakness, fibers with internalized nuclei >3%, hypertrophic/splitting fibers, ragged red fibers, whorled/ring fibers, and eosinophils infiltration as well as MHC-I and MAC staining, Fisher's exact two-tailed test was applied for pairwise comparisons among the three subgroups. Similarly, Fisher's exact two-sided test was used to compare perimysial CD8, endomysial and perimysial CD20 infiltration between LGMDR1 and LGMDR2 patients. For the remaining categorical variables, such as myonecrosis on HE staining and other inflammatory cell infiltrations across the three groups, the chi-square test was utilized. For variables conforming to a normal distribution, the unpaired t test was employed; otherwise, the Mann-Whitney U test was used. The above statistical analyses were carried out using GraphPad Prism version 9.5.0. A p value less than 0.05 was considered to indicate statistical significance.

Due to the similarity of clinical, serological, and pathological characteristics and the limited number of samples in each subgroup, LGMDR1 and LGMDR2 were merged into a combined group as LGMD in this model. A multivariate least absolute shrinkage and selection operator (Lasso) logistic regression analysis was applied to identify significant risk factors among the clinical, laboratory, and histopathological characteristics for predicting the probability of LGMD. Given that the reduction of sarcolemmal dysferlin was only useful for the differential diagnosis between LGMDR2 and IIM, we excluded this variable from the risk factors to ensure the universality of the differential diagnosis model.

Although the synchronous Mb/CK value was missing in the majority of patients (82/117, 70.1%), there is a high differential diagnostic efficiency of this ratio, with a cut-off value of 0.18 among the remaining patients (Fig. 1C). In order to involve the synchronous Mb/CK value into the differential diagnostic model, we created a categorical variable for the indicator Mb/CK, which includes three situations: (1) Mb/CK is missing, (2) Mb/CK is less than 0.18, and (3) Mb/CK is over 0.18. If Mb/CK is lower than 0.18, this variable is assigned a value of 1; conversely, when Mb/CK is missing or higher than 0.18, it is assigned a value of 0.

The significant risk factors identified by the Lasso algorithm were initially integrated to establish a nomogram prediction model. A decision tree model was further refined to provide a more user-friendly visualization tool. To mitigate the risk of overfitting and enhance model simplicity, stepwise regression was employed when constructing the nomogram, concurrently restricting the

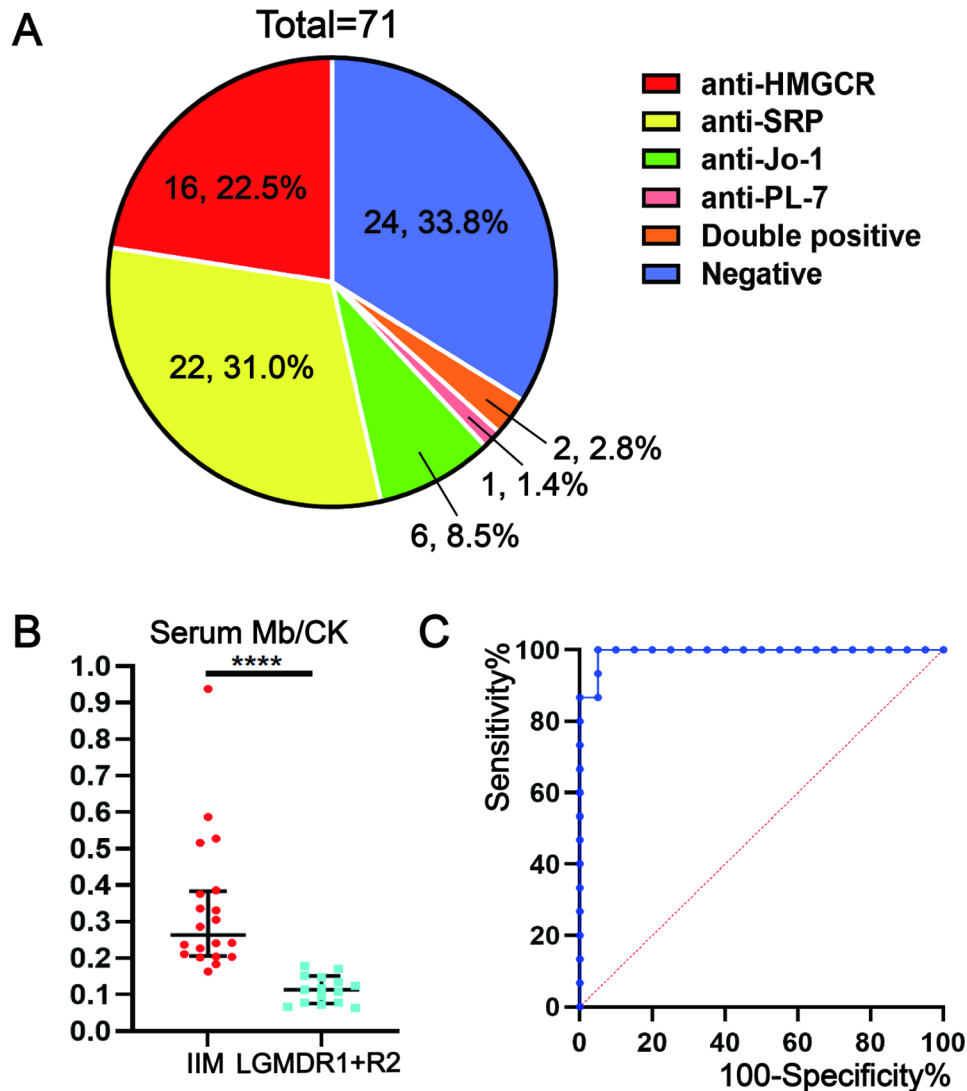


Fig. 1 Serological examinations **A** Distribution of myositis-specific autoantibodies in IIM patients. **B** The ratio of synchronous Mb (ng/ml) to CK (U/L) was significantly higher in IIM patients than in both LGMDR1 and LGMDR2 individuals. **C** ROC analysis indicated a high differential diagnostic efficiency of the ratio of synchronous Mb/CK between the IIM subgroup and the LGMD subgroups, with a cutoff value of 0.18, achieving a sensitivity of 100% and a specificity of 95% ($p < 0.0001$)

maximum depth of the decision tree. Additionally, five-fold cross-validation and bootstrapping techniques for internal validation were applied to assess the predictive capabilities of the two models. The discriminative performance of the two differential diagnostic models was evaluated by accuracy, specificity, sensitivity, and the area under the ROC curve (AUC). All computational analyses were conducted using R and Python softwares.

Results

Clinical and laboratory characteristics

The clinical characteristics of IIM, LGMDR2 and LGMDR1 patients were collected and are summarized in Table 1. Compared with LGMDR1 and LGMDR2 patients, IIM patients had an older age of disease

onset and hospital visit, and a shorter disease duration ($P < 0.0001$). Cervical muscle weakness, especially cervical flexor involvement, was more common in IIM patients. Bulbar symptoms were observed only in IIM individuals, but there was no statistically significant difference compared to those in the LGMD subgroups, which might be related to the limited number of patients. There was no significant difference in sex ratio, myalgia, or distal muscle weakness between the different subgroups.

Regarding laboratory examinations, the CK level was markedly elevated in all three subgroups, especially in LGMDR2 patients, while the simultaneous Mb level was statistically higher in IIM patients. The ratio of synchronous Mb (ng/ml)/CK (U/L) was significantly higher in

Table 1 Clinical and laboratory characteristics between different of subgroups of patients

	IIM (n = 71)	LGMDR2 (n = 24)	LGMDR1 (n = 22)	p1 value	p2 value	p3 value
Age of onset (years)	54 (49, 60)	24 (19, 37)	23.1 ± 9.8	< 0.0001	< 0.0001	0.190
Age of visit (years)	55 (49, 61)	33.6 ± 13.2	29.4 ± 13.7	< 0.0001	< 0.0001	0.297
Disease duration (months)*	4 (2, 12)	36 (20, 89)	36 (24, 102)	< 0.0001	< 0.0001	0.657
Sex, female (n, %)	48, 66.2%	14, 58.3%	12, 54.5%	0.623	0.326	> 0.9999
Cervical extensor weakness (n, %)	21, 29.6%	1, 4.2%	2, 9.5%	0.011	0.086	0.592
Cervical flexor weakness (n, %)	31, 43.7%	1, 4.2%	1, 4.8%	0.0003	0.0006	> 0.9999
Myalgia (n, %)	14, 19.7%	2, 8.3%	3, 13.6%	0.343	0.753	0.652
Bulbar symptoms (n, %)	10, 14.1%	0	0	0.061	0.109	—
Distal weakness (n, %)	31, 43.7%	9, 37.5%	9, 42.9%	0.640	> 0.9999	0.767
CK (U/L)	3470 (1869, 7613)	6921 (3605, 10266)	3247 (1727, 5043)	0.022	0.375	0.002
Synchronous Mb (ng/ml)	982 (729, 1566) (n = 20)	335 (191, 773) (n = 8)	315 (241, 395) (n = 7)	0.016	0.0004	0.694
Ratio of Mb to CK	0.264 (0.207, 0.384)	0.113 ± 0.040	0.116 ± 0.038	< 0.0001	< 0.0001	0.884

Abbreviation IIM: idiopathic inflammatory myopathy; LGMD: limb-girdle muscular dystrophy; CK: creatine kinase; Mb: myoglobin * time from onset to muscle biopsy; p1 value: IIM vs. LGMDR2; p2 value: IIM vs. LGMDR1; p3 value: LGMDR1 vs. LGMDR2

patients with IIM compared to those with LGMDR1 and LGMDR2 ($P < 0.0001$, Fig. 1B). ROC analysis indicated a high differential diagnostic efficiency of the ratio of synchronous Mb/CK with a cutoff value of 0.18, achieving a sensitivity of 100% and a specificity of 95% ($p < 0.0001$, Fig. 1C). For the MSA profiles of the IIM subgroup, 16 patients tested positive for anti-HMGCR antibodies, 22 patients for anti-SRP antibodies, 6 patients for anti-Jo-1 antibodies, 1 patient for anti-PL-7 antibody and 2 patients for double MSAs (anti-MDA-5/anti-HMGCR antibodies and anti-SRP/anti-PL-12 antibodies, respectively). The other 24 IIM patients tested negative for any known MSA (Fig. 1A).

Muscle pathology

The histopathological features of IIM, LGMDR2, and LGMDR1 patients are summarized in Table 2. There was no significant difference in myofiber necrosis among the 3 subgroups, while increased myofibers with internalized nuclei (Fig. 2A) were more common in the LGMD subgroups. Despite the younger age at which muscle biopsies were conducted, RRFs were more frequently observed in the LGMD subgroups, especially in LGMDR2 patients (Fig. 2B). Hypertrophic/splitting fibers (33.3%), and whorled/ring fibers (42.9%) were most commonly observed in LGMDR1 patients (Fig. 2E). Although there was no significant difference, eosinophils were observed only in IIMs and LGMDR1 patients but not in LGMDR2 patients (Fig. 2D).

According to the immunohistochemistry results, desferlin expression on the sarcolemma was decreased or absent not only in LGMDR2 individuals but also in two anti-HMGCR IIM patients (Fig. 2C, G). The infiltration of CD3⁺ T lymphocytes in the endomysium and perimysium was statistically significantly higher in individuals

with IIM, compared to those with LGMDR2. However, no significant differences were found in the infiltration of CD8⁺ T lymphocytes, CD20⁺ B cells, or CD68⁺ macrophages between IIM and LGMD patients. MHC-I expression and MAC deposition on nonnecrotic myofiber sarcolemma were common in all three subgroups, with a greater proportion in IIM and LGMDR2 individuals. However, the prevalence of diffuse MHC-I expression was distinctly higher in IIM patients compared to those in the two LGMD subgroups (Fig. 2F, I). MAC deposition on capillaries could only be detected in 4 (5.6%) IIM patients (Fig. 2H). MxA was negative in all patients.

Development of the differential diagnostic models

Following stepwise logistic regression with Lasso and decision tree pruning, only four significant indices were identified as independent risk factors, as the inclusion of additional variables did not yield any further significant improvement in accuracy of this model. These variables included age of onset, cervical flexor weakness, the synchronous Mb/CK value and diffuse MHC-I expression.

Involved into a multivariate logistic regression, their estimators were -0.267, -5.599, -3.391, and 6.669, respectively. The constant was 10.886. The standard errors and P values are presented in Supplemental Table 1. The final nomogram and decision tree were shown in Figs. 3 and 4, respectively.

Evaluation of the differential diagnosis models

The calibration plot of the nomogram model, based on the results of bootstrapping technique, exhibited a closer alignment with the diagonal dashed line, which indicated an ideal evaluation by a perfect model (Supplementary Fig. 1A). After the data were randomly divided into training and testing sets at a 7:3 ratio, the ROC curve

Table 2 Comparison of the histopathological characteristics between different subgroups of patients

	IIM (n = 71)			LGMDR2 (n = 24)			LGMDR1 (n = 21)			p1 value	p2 value	p3 value
	0	1	2	0	1	2	0	1	2			
Score	0	1	2	0	1	2	0	1	2	0.159	0.318	0.652
Myonecrosis	2, 2.8%	34, 47.9%	35, 49.3%	2, 8.3%	15, 62.5%	7, 29.2%	3, 14.3%	14, 66.7%	4, 19.0%	< 0.0001	0.0008	0.730
Fibers with internalized nuclei > 3%	21, 29.6%			19, 79.2%			15, 71.4%			0.262	< 0.0001	0.038
Hypertrophic/splitting fibers	14, 19.7%			8, 33.3%			14, 66.7%			0.017	0.117	0.746
Ragged red fibers	6, 8.5%			7, 29.2%			5, 23.8%			0.085	0.001	0.226
Whorled/ring fibers	7, 9.9%			6, 25.0%			9, 42.9%			0.325	0.377	0.094
Eosinophils infiltration	5, 7.0%			0			3, 14.3%					
Score	0	1	2	0	1	2	0	1	2			
Endomysial CD3 infiltration	5, 7.0%	29, 40.8%	37, 52.1%	0	18, 75.0%	6, 25.0%	1, 4.8%	11, 52.4%	9, 42.9%	0.012	0.637	0.212
Perimysial CD3 infiltration	17, 23.9%	34, 47.9%	20, 28.2%	12, 50.0%	0	0	4, 19.0%	14, 66.7%	3, 14.3%	0.005	0.284	0.030
Endomysial CD8 infiltration	15, 21.1%	34, 47.9%	22, 31.0%	8, 33.3%	14, 58.3%	2, 8.3%	4, 19.0%	12, 57.1%	5, 23.8%	0.077	0.742	0.275
Perimysial CD8 infiltration	37, 52.1%	27, 38.0%	7, 9.9%	18, 75.0%	6, 25.0%	0	9, 42.3%	12, 57.1%	0	0.088	0.154	0.037
Endomysial CD20 infiltration	66, 93.0%	4, 5.6%	1, 1.4%	23, 95.8%	1, 4.2%	0	20, 95.2%	1, 4.8%	0	0.808	0.849	> 0.999
Perimysial CD20 infiltration	65, 91.5%	5, 7.0%	1, 1.4%	24, 100.0%	0	0	20, 95.2%	1, 4.8%	0	0.339	0.799	0.467
Endomysial CD68 infiltration	0	15, 21.1%	56, 78.9%	1, 4.2%	5, 20.8%	18, 75.0%	0	4, 19.0%	17, 81.0%	0.224	> 0.999	0.624
Perimysial CD68 infiltration	1, 1.4%	39, 54.9%	31, 43.7%	2, 8.3%	9, 37.5%	13, 54.2%	0	11, 52.4%	10, 47.6%	0.121	0.830	0.301
Positive MHC-I expression	65, 91.5%			19, 79.2%			9, 42.9%			0.138	< 0.0001	0.016
Diffuse MHC-I expression	35, 49.3%			0			3, 14.3%			< 0.0001	0.005	0.094
MAC deposition on sarcolemma	61, 85.9%			22, 91.7%			13, 61.9%			0.724	0.026	0.029
MAC deposition on capillaries	4, 5.6%			0			0			0.569	0.570	—

Abbreviation: IIM: Idiopathic inflammatory myopathy; LGMD: limb-girdle muscular dystrophy; MHC-I: major histocompatibility complex class-I; MAC: membrane attack complex; p1 value: IIM vs. LGMDR2, p2 value: IIM vs. LGMDR1, p3 value: LGMDR1 vs. LGMDR2

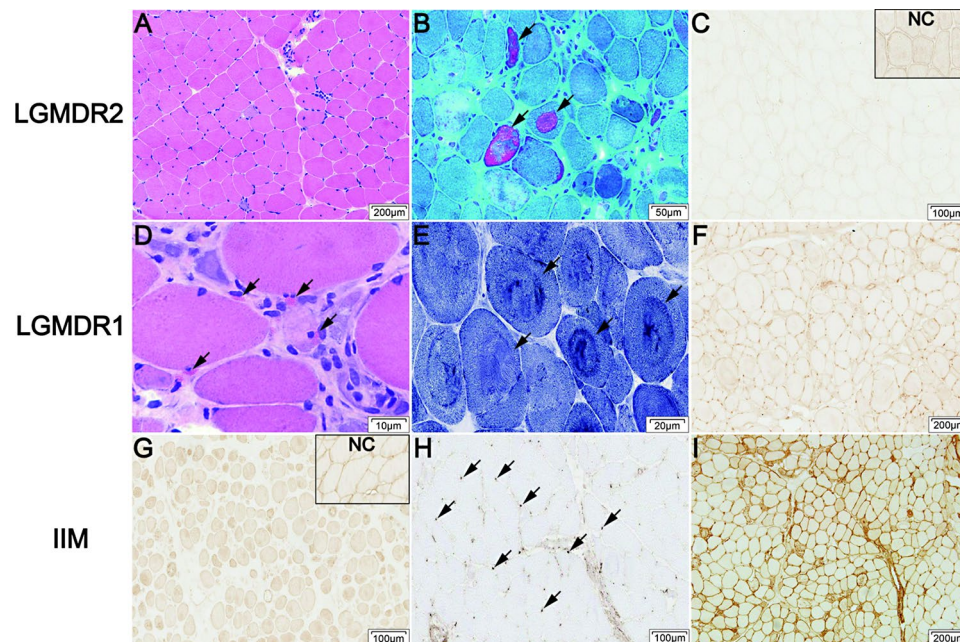


Fig. 2 Muscle pathology **A-C** LGMDR2: **(A)** Increased fibers with internalized nuclei (HE staining); **(B)** Typical ragged red fibers (MGT staining, arrows); **(C)** Significantly reduced dysferlin immunostaining compared with the contemporaneous normal control. **D-F** LGMDR1: **(D)** Eosinophils scattered in the endomysium (HE staining, arrows); **(E)** Typical whorled fibers (NADH staining, arrows). **(F)** Negative MHC-I expression. **G-I** IIM: **(G)** Dysferlin immunostaining was also significantly reduced in anti-HMGCR patients. **(H)** MAC deposition on capillaries could be detected in an MSA-negative IIM patient (arrows). **(I)** Diffuse MHC-I expression in an anti-HMGCR-positive IIM patient

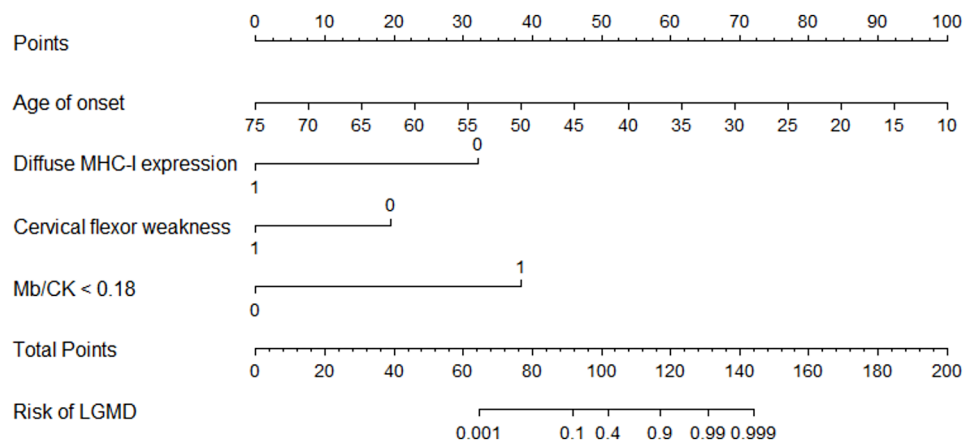


Fig. 3 A nomogram prediction model for identifying LGMD. There are four significant independent indicators included in this differential diagnosis model: age of onset, diffuse MHC-I expression, cervical flexor weakness, and the ratio of synchronous Mb/CK. For the variable Mb/CK < 0.18, if the value Mb/CK is lower than 0.18, the corresponding value is set to 1, while the value of 0 represents that the Mb/CK is missing or bigger than 0.18. In addition, if cervical flexor weakness or diffuse MHC-I expression is confirmed, the corresponding value is set to 1; otherwise, the value is set to 0. For each risk factor, a score was determined by reading the values of each risk factor on the ruler superimposed over its respective graph line. An aggregate score, computed by summing the individual scores for each risk factor, yields the likelihood of LGMD prediction

was generated for the test set, yielding an area under the curve (AUC) was 0.963 (Supplementary Fig. 1B). Moreover, the predictive performance of this model was also evaluated by K-fold cross-validation ($K=5$). The AUC from the stratified 5-fold cross-validation analysis was 0.973. The cross-validation results indicated that this model exhibited a sensitivity of 92.920%, a specificity of 92.926%, a positive predictive value of 89.325%, a

negative predictive value of 95.783% and a balanced accuracy of 92.923%.

Regarding the decision tree analysis, employing a consistent ratio for the training and testing sets, as previously described, resulted in an AUC of 0.934. When employing a stratified 5-fold cross-validation approach, the AUC was determined to be 0.910. This model demonstrated

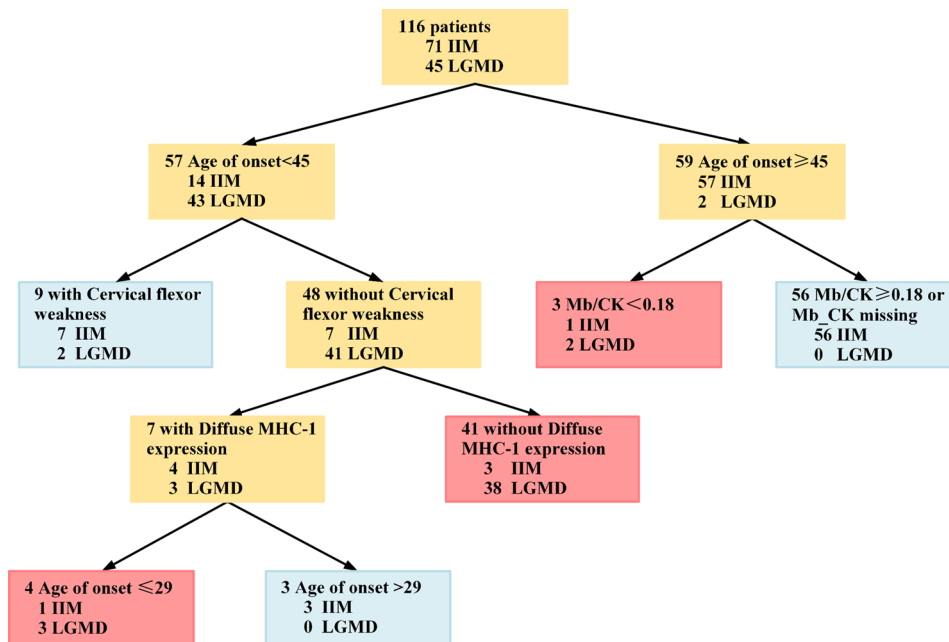


Fig. 4 A pruned prediction model was developed using four variables: age of onset, cervical flexor weakness, Mb/CK, and diffuse MHC-I expression. The red box indicates that this group of patients will be ultimately classified as LGMD in the decision tree model, while the blue box represents patients who are diagnosed as IIM

a sensitivity of 86.667%, a specificity of 85.905%, and an overall accuracy of 86.232%.

Discussion

In this study, we summarized and compared the characteristics of the three most common prototypes of necrotizing myopathies, which are easily confused with each other clinically. We further developed a convenient and reliable nomograph model and a decision tree to distinguish between patients with IIM and LGMD based on four easily accessible indicators.

Clinically, a younger age of onset and a longer disease duration usually indicate a diagnosis of LGMD other than IIM. However, this is not always true, as there are some IIM patients with a juvenile age of onset or a chronic slowly progressive course who are most easily misdiagnosed as having heterogeneous muscular dystrophy [8, 15, 16]. Consistent with previous studies, our study highlighted that the involvement of cervical muscles, particularly the weakness of cervical flexor muscles could serve as a distinguishing characteristic between IIM and LGMD, as cervical muscles are rarely affected in LGMD patients both in clinical assessment and on muscle MRI [17–19]. Although there have been many studies comparing the clinical and pathological characteristics between different types of IIM and MD [8–10, 15, 20, 21], IMNM is the most frequent subtype of IIM that needs to be distinguished from LGMD, as more than half of the IIM patients included in our study were found to possess the anti-SRP or anti-HMGCR antibodies. This could

be attributed to the clinical and laboratory similarities between IMNM and LGMD [9].

Based on the findings of laboratory examinations, CK was markedly elevated in all three subgroups. Therefore, this value was not effective enough for differentiating between IIM and LGMD. Interestingly, we observed that the simultaneous Mb levels were statistically lower in both LGMDR1 and LGMDR2 patients compared to IIM individuals, resulting in a significantly lower ratio of Mb (ng/ml) to CK (U/L) in the two LGMD subgroups. Although simultaneous Mb levels were detected in 35 patients, the ratio of synchronous Mb to CK, with a cut-off value of 0.18, showed a high differential diagnostic efficiency. This result indicates that it is a highly reliable and convenient parameter for differentiating between the IIM and LGMD patients. Presumably, both the serum Mb and CK levels are indicative of changes in muscle permeability or other causes of muscle damage. However, Mb has much faster elimination kinetics than CK, as proven in patients with acute myocardial infarction and rhabdomyolysis [22], which might be partially attributable to the different molecular masses of these two sarcoplasmic proteins. Therefore, we hypothesized that Mb might tend to reach a lower level in LGMD patients during a long chronic disease course, while it could persist at a relatively high level in those with IIM who are still in the active phases of a shorter disease course.

Regarding muscle pathology, chronic myopathic features, such as increased fibers with internalized nuclei, whorled or ring fibers, and hypertrophic/splitting fibers,

were more commonly observed in the LGMD subgroups, which has also been noted in previous studies [15, 23]. In addition, the occurrence of RRFs in the two LGMD subgroups, especially in LGMDR2 patients, was more frequent than that in IIM patients. In fact, mitochondrial dysfunction has been indicated in LGMDR2 and several other LGMD subtypes [24–28]. In IIM, RRFs and COX-deficient myofibers are usually observed in inclusion body myositis, polymyositis, and the perifascicular region of dermatomyositis [29, 30], but are seldom reported in IMNM, which constitute the majority of IIM in this cohort. The number of RRFs increases with normal aging [30]. Given that the patients with LGMD were significantly younger than those with IIM, our study indicated that when RRFs were noted in a patient with necrotizing myopathy at a younger age, a diagnosis of LGMD rather than IMNM was more likely to be present.

Immunohistochemistry for inflammatory markers and the aberrant sarcolemmal protein is often used to differentiate between IIM and MD. Consistent with previous studies [8, 9], the similarity of lymphocytes infiltration in these patients made it difficult to be used as a distinguishing variable for differential diagnosis. Likewise, the presence of scattered eosinophils was nonspecific to either hereditary or inflammatory myopathies, in line with the findings of a prior study [31]. Reduced dysferlin expression on the sarcolemma of myofibers, as identified by immunohistochemistry, is a common method used to differentiate LGMDR2 from IIM and other diseases. However, reduced dysferlin immunostaining may also be secondary to many other inherited or acquired conditions, such as dystrophinopathy, calpainopathy, sarcoglycanopathy, caveolinopathy or immune-mediated rippling muscle disease with AChR-antibody positive myasthenia gravis [32–36]. Our study is the first to report that dysferlin immunostaining was reduced in two anti-HMGCR patients, which could be attributable to secondary inflammatory damage to the sarcolemma of myofibers. This finding suggested that the possibility of a treatable IIM could not be excluded due to reduced dysferlin immunostaining on muscle pathology. In addition, MHC-I expression has routinely been included as a diagnostic criterion for IIM [37]. A recent study reported that positive MHC-I immunostaining was more frequent in IIM than in inherited myopathies [38]. In the present cohort, abnormal MHC-I immunostaining was common in all three subgroups. However, diffuse MHC-I expression was more frequently observed in the IIM subgroup than in either LGMDR1 or LGMDR2 patients. Therefore, we hypothesized that only the diffuse pattern of MHC-I expression could be used as an indicator for differentiating IIM from LGMD.

To date, many studies have focused on comparing various subtypes of MD and IIM, but the previous intricate

results still make it difficult to render a precise judgment in clinical practice [8–10, 15, 20, 21, 38]. In this study, we developed two differential diagnostic models—a nomogram and a decision tree—both of which exhibited high sensitivity, specificity and predictive efficiency in distinguishing between patients with LGMD and IIM. Four variables, namely age of onset, cervical flexor weakness, synchronous Mb/CK value and diffuse MHC-I expression, were identified as independent risk factors. All of these parameters can be easily and uniformly evaluated by the clinicians and pathologists. Specifically, the nomogram model suggested that the ratio of synchronous Mb (ng/ml) to CK (U/L) could have valuable potential for distinguishing LGMD from IIM patients. For example, if a patient with an age of onset of 22 years (equivalent to a model score of 80) exhibits a synchronous Mb/CK ratio of less than 0.18 (equivalent to a model score of 40), the likelihood of developing LGMD exceeds 0.90, with a cumulative score of 120 points. Similarly, for a 45-year-old patient with a Mb/CK ratio lower than 0.18, if there is no diffuse MHC-I expression and cervical flexor weakness, the probability of developing LGMD is greater than 0.95 with a cumulative score of 135 points. At last, we recommend that Mb should be routinely detected with CK in patients with undiagnosed necrotizing myopathy. To emphasize, both the Mb and CK values should be detected simultaneously before any medical intervention, as both can be significantly affected by immunotherapy.

Our study has several limitations. Firstly, this was a retrospective analysis from a single neuromuscular center, with a limited number of patients and disease phenotypes, inevitable recall and referral bias will contribute to the findings. And the enrolled IIMs patients in this study are likely more frequently seen in a neuromuscular center, and might differ from those typically encountered in rheumatology, respiratory medicine, or dermatology settings. Secondly, muscle MRI data were not included for comparison in this study, as only a few patients underwent MRI scans and it is difficult to quantify the manifestations on MRI. Thirdly, MSAs were detected only by immunoblotting and not confirmed by immunoprecipitation. However, the antibody results and the clinicopathological profiles were in accordance with each other in our IIM patients. Finally, external validation of the prediction models is difficult to complete as the synchronous Mb and CK value was collected in a limited number of patients. However, we found that the synchronous Mb/CK value showed a consistent trend in other types of MD, such as Becker muscular dystrophy or LGMDR9 (data not shown), which needs further confirmation at other NMD centers with larger samples.

Conclusion

In conclusion, we developed two practical differential diagnosis models for LGMD and IIM based on the analysis of four accessible indicators, including the age of onset, cervical flexor weakness, the ratio of synchronous Mb/CK values and diffuse MHC-I expression. A patient with necrotizing myopathy, characterized by a younger age of onset, absence of cervical flexor weakness, lower Mb/CK value and lack of diffuse MHC-I expression, is more commonly suggestive of LGMD. Otherwise, it is more indicative of IIM. Further studies with larger samples are still needed to refine the predictive efficiency of the differential diagnostic models for these conditions.

Abbreviations

LGMD	Limb-Girdle Muscular Dystrophy
IIM	Idiopathic Inflammatory Myopathy
Mb	Myoglobin
CK	Creatine Kinase
MSA	Myositis-Specific Autoantibody
MRI	Magnetic Resonance Imaging
IMNM	Immune-Mediated Necrotizing Myopathy
DM	Dermatomyositis
sIBM	sporadic Inclusion Body Myositis
MD	Muscular Dystrophy
NMD	Neuromuscular Disorder
ROC	Receiver Operating Characteristic
AUC	Area Under the ROC Curve
ARS	Anti-Aminoacyl tRNA Synthetase
HE	Hematoxylin and Eosin
NADH	Nicotinamide Adenine Dinucleotide Tetrazolium Reductase
COX	Cytochrome Oxidase
MGT	Modified Gomori Trichrome
MxA	Myxovirus Resistance Protein
MHC-I	Major Histocompatibility Complex Class-I
MAC	Membrane Attack Complex

Supplementary Information

The online version contains supplementary material available at <https://doi.org/10.1186/s13075-024-03458-8>.

Supplementary Material 1

Supplementary Material 2: Supplementary Fig. 1: Results of model prediction performance evaluation **A** The bootstrapping-validated calibration plot showed a closer alignment with the diagonal dashed line, which represents an ideal evaluation by a perfect model. **B** After the data were randomly divided into training and testing sets at a 7:3 ratio, a receiver operating characteristic (ROC) curve was obtained for the test set, the area under the curve (AUC) of which was 0.963.

Acknowledgements

We would like to thank all the patients involved in the study.

Author contributions

GW: Conceptualization, methodology, data curation, writing-original and draft preparation. LF: Methodology and statistical analysis; TD, evaluation of the muscle pathology; LZ, KS, YH, PL: Validation and statistical analysis. CY conceptualization, methodology, writing, and funding acquisition; BZ, evaluation of the muscle pathology and reviewing, editing of the manuscript.

Funding

This work was supported by the National Natural Science Foundation of China (grant numbers. 82071412, grant numbers. 82201556, and grant numbers. 82171395), the Natural Science Foundation of Shandong Province

(grant numbers. ZR2023QH364 and grant numbers. ZR2021QH120), the Qingdao Natural Science Foundation (Project 24-2-2-zrjj-104-jch); the Qingdao Key Health Discipline Development Fund and the Qingdao Clinical Research Center for Rare Diseases of Nervous Systems (grant numbers. 22-3-7-lczx-3-nsh).

Data availability

No datasets were generated or analysed during the current study.

Declarations

Ethics approval and consent to participate

This study was approved by the Ethics Committee of Qilu Hospital (Qingdao), Shandong University, China (KYL-KS-2022054). Written consent for muscle biopsy, laboratory tests and article publication was obtained from all the patients or their parents in the present study. The study was performed in accordance with the Declaration of Helsinki.

Consent for publication

Not applicable.

Competing interests

The authors declare no competing interests.

Author details

¹Department of Neurology, Shandong Key Laboratory of Mitochondrial Medicine and Rare Diseases, Research Institute of Neuromuscular and Neurodegenerative Diseases, Qilu Hospital of Shandong University, Jinan, Shandong 250012, China

²School of Finance, Southwestern University of Finance and Economics, Chengdu 611130, China

³Department of Rheumatology, Qilu Hospital of Shandong University, Jinan, Shandong 250012, China

⁴Department of Central Laboratory, Qilu Hospital (Qingdao), Cheeloo College of Medicine, Shandong University, 758 Hefei Road, Qingdao, Shandong 266035, China

⁵Qilu Hospital (Qingdao), Cheeloo College of Medicine, Shandong University, Qingdao, Shandong 266035, China

Received: 9 October 2024 / Accepted: 8 December 2024

Published online: 19 December 2024

References

1. Töpf A, Johnson K, Bates A, Phillips L, Chao KR, England EM, et al. Sequential targeted exome sequencing of 1001 patients affected by unexplained limb-girdle weakness. *Genet Med*. 2020;22(9):1478–88.
2. Nallamilli BRR, Chakravorty S, Kesari A, Tanner A, Ankala A, Schneider T, et al. Genetic landscape and novel disease mechanisms from a large LGMD cohort of 4656 patients. *Ann Clin Transl Neurol*. 2018;5(12):1574–87.
3. McHugh NJ, Tansley SL. Autoantibodies in myositis. *Nat Rev Rheumatol*. 2018;14(5):290–302.
4. Betteridge Z, McHugh N. Myositis-specific autoantibodies: an important tool to support diagnosis of myositis. *J Intern Med*. 2016;280(1):8–23.
5. Tansley SL, Simou S, Shaddick G, Betteridge ZE, Almeida B, Gunawardena H, et al. Autoantibodies in juvenile-onset myositis: Their diagnostic value and associated clinical phenotype in a large UK cohort. *J Autoimmun*. 2017;84:55–64.
6. Li S, Li W, Jiang W, He L, Peng Q, Wang G, et al. The Efficacy of Tocilizumab in the Treatment of Patients with Refractory Immune-Mediated Necrotizing Myopathies: An Open-Label Pilot Study. *Front Pharmacol*. 2021;12:635654.
7. Oddis CV, Rockette HE, Zhu L, Koontz DC, Lacomis D, Venturupalli S, et al. Randomized Trial of Tocilizumab in the Treatment of Refractory Adult Poly-myositis and Dermatomyositis. *ACR Open Rheumatol*. 2022;4(11):983–90.
8. Mamurova G, Katz JD, Jones RV, Targoff IN, Lachenbruch PA, Jones OY, et al. Clinical and laboratory features distinguishing juvenile polymyositis and muscular dystrophy. *Arthritis Care Res (Hoboken)*. 2013;65(12):1969–75.
9. Yang M, Ji S, Xu L, Zhang Q, Li Y, Gao H, et al. The Clinicopathological Distinction between Immune-Mediated Necrotizing Myopathy and Limb-Girdle

- Muscular Dystrophy R2: Key Points to Prevent Misdiagnosis. *J Clin Med*. 2022;11(21):6566.
10. Becker N, Moore SA, Jones KA. The inflammatory pathology of dysferlinopathy is distinct from calpainopathy, Becker muscular dystrophy, and inflammatory myopathies. *Acta Neuropathol Commun*. 2022;10(1):17.
 11. Mammen AL. Which nonautoimmune myopathies are most frequently misdiagnosed as myositis? *Curr Opin Rheumatol*. 2017;29(6):618–22.
 12. Vangstad M, Bjornaas MA, Jacobsen D. Rhabdomyolysis: a 10-year retrospective study of patients treated in a medical department. *Eur J Emerg Med*. 2019;26(3):199–204.
 13. Wedderburn LR, Varsani H, Li CK, Newton KR, Amato AA, Banwell B, et al. International consensus on a proposed score system for muscle biopsy evaluation in patients with juvenile dermatomyositis: a tool for potential use in clinical trials. *Arthritis Rheum*. 2007;57(7):1192–201.
 14. Tanboon J, Inoue M, Saito Y, Tachimori H, Hayashi S, Noguchi S, et al. Dermatomyositis: Muscle Pathology According to Antibody Subtypes. *Neurology*. 2022;98(7):e739–49.
 15. Mohassel P, Landon-Cardinal O, Foley AR, Donkervoort S, Pak KS, Wahl C, et al. Anti-HMGCR myopathy may resemble limb-girdle muscular dystrophy. *Neurol Neuroimmunol Neuroinflamm*. 2018;6(1):e523.
 16. Liang WC, Uruha A, Suzuki S, Murakami N, Takeshita E, Chen WZ, et al. Pediatric necrotizing myopathy associated with anti-3-hydroxy-3-methylglutaryl-coenzyme A reductase antibodies. *Rheumatology (Oxford)*. 2017;56(2):287–93.
 17. Watanabe Y, Uruha A, Suzuki S, Nakahara J, Hamanaka K, Takayama K, et al. Clinical features and prognosis in anti-SRP and anti-HMGCR necrotizing myopathy. *J Neurol Neurosurg Psychiatry*. 2016;87(10):1038–44.
 18. Wang Y, Zhao Y, Yu M, Wei L, Zhang W, Wang Z, et al. Clinicopathological and circulating cell-free DNA profile in myositis associated with anti-mitochondrial antibody. *Ann Clin Transl Neurol*. 2023;10(11):2127–38.
 19. Díaz J, Woudt L, Suazo L, Garrido C, Caviedes P, Cárdenas AM, et al. Broadening the imaging phenotype of dysferlinopathy at different disease stages. *Muscle Nerve*. 2016;54(2):203–10.
 20. Benveniste O, Romero NB. Myositis or dystrophy? Traps and pitfalls. *Presse Med*. 2011;40(4 Pt 2):e249–55.
 21. Xu C, Chen J, Zhang Y, Li J. Limb-girdle muscular dystrophy type 2B misdiagnosed as polymyositis at the early stage: Case report and literature review. *Med (Baltim)*. 2018;97(21):e10539.
 22. Lappalainen H, Tiula E, Uotila L, Mänttari M. Elimination kinetics of myoglobin and creatine kinase in rhabdomyolysis: implications for follow-up. *Crit Care Med*. 2002;30(10):2212–15.
 23. Fanin M, Nardetto L, Nascimbeni AC, Tasca E, Spinazzi M, Padoan R, et al. Correlations between clinical severity, genotype and muscle pathology in limb girdle muscular dystrophy type 2A. *J Med Genet*. 2007;44(10):609–14.
 24. Bisceglia L, Zoccollella S, Torraco A, Piemontese MR, Dell'Aglio R, Amati A, et al. A new locus on 3p23-p25 for an autosomal-dominant limb-girdle muscular dystrophy, LGMD1H. *Eur J Hum Genet*. 2010;18(6):636–41.
 25. Justel M, Jou C, Sariego-Jamardo A, Juliá-Palacios NA, Ortez C, Poch ML, et al. Expanding the phenotypic spectrum of TRAPPC11-related muscular dystrophy: 25 Roma individuals carrying a founder variant. *J Med Genet*. 2023;60(10):965–73.
 26. Vázquez J, Lefeuvre C, Escobar RE, Luna Angulo AB, Miranda Duarte A, Delia Hernandez A, et al. Phenotypic Spectrum of Myopathies with Recessive Anoctamin-5 Mutations. *J Neuromuscul Dis*. 2020;7(4):443–51.
 27. Gayathri N, Alefia R, Nalini A, Yasha TC, Anita M, Santosh V, et al. Dysferlinopathy: spectrum of pathological changes in skeletal muscle tissue. *Indian J Pathol Microbiol*. 2011;54(2):350–4.
 28. Liu F, Lou J, Zhao D, Li W, Zhao Y, Sun X, et al. Dysferlinopathy: mitochondrial abnormalities in human skeletal muscle. *Int J Neurosci*. 2016;126(6):499–509.
 29. Chariot P, Ruet E, Authier FJ, Labes D, Poron F, Gherardi R. Cytochrome c oxidase deficiencies in the muscle of patients with inflammatory myopathies. *Acta Neuropathol*. 1996;91(5):530–6.
 30. Rifai Z, Welle S, Kamp C, Thornton CA. Ragged red fibers in normal aging and inflammatory myopathy. *Ann Neurol*. 1995;37(1):24–9.
 31. Schröder T, Fuchss J, Schneider I, Stoltenburg-Didinger G, Hanisch F. Eosinophils in hereditary and inflammatory myopathies. *Acta Myol*. 2013;32(3):148–53.
 32. Piccolo F, Moore SA, Ford GC, Campbell KP. Intracellular accumulation and reduced sarcolemmal expression of dysferlin in limb-girdle muscular dystrophies. *Ann Neurol*. 2000;48(6):902–12.
 33. Hermanová M, Zapletalová E, Sedláčková J, Chrobáková T, Letocha O, Kroupová I, et al. Analysis of histopathologic and molecular pathologic findings in Czech LGMD2A patients. *Muscle Nerve*. 2006;33(3):424–32.
 34. Tateyama M, Aoki M, Nishino I, Hayashi YK, Sekiguchi S, Shiga Y, et al. Mutation in the caveolin-3 gene causes a peculiar form of distal myopathy. *Neurology*. 2002;58(2):323–5. Erratum in: *Neurology* 2002;58(5):839. Itoyama Y [corrected to Itoyama Y].
 35. Gangfuß A, Hentschel A, Heil L, Gonzalez M, Schönecker A, Depienne C, et al. Proteomic and morphological insights and clinical presentation of two young patients with novel mutations of BVES (POPDC1). *Mol Genet Metab*. 2022;136(3):226–37.
 36. Schoser B, Jacob S, Hilton-Jones D, Müller-Felber W, Kubisch C, Claus D, et al. Immune-mediated rippling muscle disease with myasthenia gravis: a report of seven patients with long-term follow-up in two. *Neuromuscul Disord*. 2009;19(3):223–8.
 37. Hoogendijk JE, Amato AA, Lecky BR, Choy EH, Lundberg IE, Rose MR, et al. 119th ENMC international workshop: trial design in adult idiopathic inflammatory myopathies, with the exception of inclusion body myositis, 10–12 October 2003, Naarden, The Netherlands. *Neuromuscul Disord*. 2004;14(5):337–45.
 38. Milisenda JC, Pinal-Fernandez I, Lloyd TE, Grau-Junyent JM, Christopher-Stine L, Corse AM, et al. The pattern of MHC class I expression in muscle biopsies from patients with myositis and other neuromuscular disorders. *Rheumatology (Oxford)*. 2023;62(9):3156–60.

Publisher's note

Springer Nature remains neutral with regard to jurisdictional claims in published maps and institutional affiliations.